Subcycle ac Stark Shift of Helium Excited States Probed with Isolated Attosecond Pulses

Michael Chini, Baozhen Zhao, He Wang, Yan Cheng, S. X. Hu, and Zenghu Chang

Phys. Rev. Lett. **109**, 073601 — Published 16 August 2012

DOI: 10.1103/PhysRevLett.109.073601

Sub-cycle AC Stark shift of helium excited states probed with isolated attosecond pulses

Michael Chini[1], Baozhen Zhao[2], He Wang[3], Yan Cheng[1], S. X. Hu[4], and Zenghu Chang[1*]

[1]*CREOL and Department of Physics, University of Central Florida, Orlando FL 32816*

[2]*Department of Physics and Astronomy, University of Nebraska-Lincoln, Lincoln NE 68588*

[3]*Lawrence Berkeley National Laboratory, Berkeley CA 94720*

[4]*Laboratory for Laser Energetics, University of Rochester, Rochester NY 14623*

[*]*Zenghu.Chang@ucf.edu*

Abstract: Recent advances in attosecond science have relied upon the nearly instantaneous response of *free* electrons to an external field. However, it is still not clear whether *bound* electrons are able to rearrange on sub-laser cycle timescales. Here, we probe the optical Stark shifts induced by a few-cycle near infrared laser field in helium bound states using isolated attosecond pulses in a transient absorption scheme and uncover a sub-cycle laser-induced energy level shift of the laser-dressed 1s3p state.

PACS codes: 78.47.jb transient absorption; 42.50.Hz Stark shift, dynamic; 32.70.Jz line shapes, widths, and shifts

The optical Stark shift[1], the shift of atomic energy levels in a light field, was first observed in 1969[2] and is a textbook example of bound electron response to a perturbing electromagnetic field[3]. According to existing theory, when a monochromatic laser with frequency ω_L is far from any atomic resonance, the optical AC Stark shift is equivalent to the quadratic DC Stark shift[1]. The energy shift ΔE_a of the state a is then proportional to the cycle-average of the laser field's square:

$$\Delta E_a = -\frac{\alpha_a(\omega_L)}{2}\left\langle \varepsilon_L(t)^2 \right\rangle = -\frac{\alpha_a(\omega_L)}{4}\varepsilon_0{}^2 = -\frac{\alpha_a(\omega_L)}{4} I_L , \qquad (1)$$

where $\varepsilon_L(t) = \varepsilon_0 \cos(\omega_L t)$ is the laser electric field. Atomic units are used throughout except where stated otherwise. The polarizability $\alpha_a = \sum_{k \neq a} \frac{\omega_{ka} |d_{ka}|^2}{\omega_{ka}^2 - \omega_L^2}$ depends on both the dipole matrix

elements d_{ka} coupling a with other states k and the detuning of the laser frequency ω_L from the resonance frequencies ω_{ka}. I_L and ε_0 are the intensity and the electric field amplitude of the monochromatic laser respectively, which are time independent.

While the AC Stark shift in Eq. 1 is *by definition* cycle-averaged, it originates from bound electron dynamics induced by the instantaneous laser electric field on the sub-optical-cycle timescale[1, 3]. In general, we can expand the time-dependent electron wavefunction of the NIR laser-dressed atom in the basis set of the field-free atom,

$$\left|\Psi_{NIR}(\mathbf{r},t)\right\rangle = \sum_k c_k(t) e^{-iE_k(t)} \left|\psi_k(\mathbf{r})\right\rangle, \tag{2}$$

where $c_k(t)$ are the time-dependent complex amplitudes of the energy eigenstates $\left|\psi_k(\mathbf{r})\right\rangle$ with energies E_k. The bound electron dynamics can therefore be described in terms of changes in the probability of finding the electron in a given state k (*magnitude* of c_k) and changes in the energy level of the state k (*phase* of c_k). This can be understood by rewriting the electron wavefunction in the following way:

$$\left|\Psi_{NIR}(\mathbf{r},t)\right\rangle = \sum_k \left|c_k(t)\right| e^{-i\int_{-\infty}^{t}[E_k+\delta E_k(t')]\mathrm{d}t'} \left|\psi_k(\mathbf{r})\right\rangle, \tag{3}$$

where $c_k(t) = \left|c_k(t)\right| e^{-i\int_{-\infty}^{t}\delta E_k(t')dt'}$. We will refer to the energy level shifts $\delta E_k(t)$ as *sub-cycle* AC Stark shifts. If the atom is initially in the state a, second-order perturbation theory yields $\left|c_k(t)\right| \approx \delta_{ka}$, and the sub-cycle Stark shift can be calculated as [3]:

$$\delta E_a(t) = -i\sum_{k\neq a} d_{ak}\varepsilon_0(t)\cos(\omega_L t) e^{i\omega_{ak}t} \int_{-\infty}^{t} d_{ka}\varepsilon_0(t')\cos(\omega_L t') e^{i\omega_{ka}t'} dt', \tag{4}$$

where the laser pulse envelope $\varepsilon_0(t)$ now depends on time. For a double-exponential pulse shape, $\varepsilon_0(t) = \varepsilon_p e^{-|t|/\tau_p}$ with pulse duration τ_p, the integral in eq. (4) can be performed analytically for multi-cycle pulses:

$$\delta E_a(t) = \frac{1}{2}\varepsilon_0(t)^2 \sum_{k\neq a}\left[\frac{\omega_{ka}\left|d_{ka}\right|^2}{\omega_{ka}^2-\omega_L^2}\cos^2(\omega_L t) - i\frac{\omega_L\left|d_{ka}\right|^2}{\omega_{ka}^2-\omega_L^2}\sin(2\omega_L t)\right]$$

$$= \frac{1}{2}\varepsilon_0(t)^2\left[\alpha_a\cos^2(\omega_L t) - i\gamma_a\sin(2\omega_L t)\right], \tag{5}$$

where $\gamma_a = \dfrac{\omega_L\left|d_{ka}\right|^2}{\omega_{ka}^2-\omega_L^2}$ specifies the sub-cycle changes in the population of a as it couples to k.

However, the instantaneous level shifts have not been directly measured experimentally. Early experiments using monochromatic or long-pulse (~ns) laser sources [4] could verify the cycle-averaged perturbation theory predictions, but lacked time resolution. More recently, "pump-probe" measurements using probe laser pulses substantially longer than the oscillation period of the Stark field revealed Stark shifts on the timescale of the laser intensity envelope with a time resolution of ~10 *fs*[5, 6]. However, even in these experiments only the cycle-averaged energy shifts could be measured, as the available probes lacked the temporal resolution to reveal the possibility of a faster response of the bound states to the laser field. Furthermore, dynamics in field-free atomic excited states evolve on characteristic timescales similar to the classical orbital periods, which are typically longer than the Stark laser cycle, and it is therefore unclear whether the sub-cycle AC Stark shifts exist.

To resolve the sub-cycle AC Stark shifts, we probe singly excited states of helium using isolated attosecond extreme ultraviolet (XUV) pulses[7] with a pulse duration nearly 20 times smaller than the near infrared (NIR) Stark laser period. The experiments were conducted using the attosecond transient absorption technique[8]. The 140 *as* pulse with spectrum covering photon energies from 20 to 30 eV and the 6 *fs* laser pulse centered at 750 nm with intensity of $\sim 3\times10^{12}$ W/cm^2 were focused together into a helium-filled gas cell with 2 mm inner diameter and a pressure-length product of ~40 torr-mm. The single isolated attosecond pulses were generated with the generalized double optical gating, which does not require the stabilization of the carrier-envelope phase[9]. The spectrum of the XUV light passing through the laser-perturbed target was measured as a function of the time delay between the attosecond pulse and femtosecond Stark field oscillation, unveiling the dynamic response of each energy level.

The helium energy levels of interest are indicated in Fig. 1(a). When a helium atom absorbs an XUV photon, electrons can be promoted by single photon absorption from the ground state to one of several singly-excited states or to the continuum, depending upon the energy of the absorbed photon. The process leaves its mark on the transmitted XUV spectrum, with absorption features indicating the positions of energy levels relative to the ground state, as depicted in Fig. 1(b). When a moderately intense laser field perturbs the atom, the effects of the laser on the atomic states can be observed through changes in the positions and shapes of the absorption features. Such a measurement benefits from the ability to study the effects of the laser on each bound state individually although several excited states are involved.

Fig. 1(c) shows the transmitted XUV spectrum as a function of the time delay between the attosecond pulse and the near infrared laser field. The experiments were performed by averaging over ~60,000 laser shots at each delay step. Changes in the carrier-envelope phase of the femtosecond laser did not smear out the time delay between the attosecond pulse and the Stark laser field within the laser cycle, as the attosecond pulse was temporally synchronized to the field oscillation of the near infrared laser[9]. The broad continuous spectrum of the isolated attosecond pulse allows us to observe a series of bound states simultaneously. "Holes" in the spectrum, indicated by the blue color, are caused by absorption as described above, with roughly half of the signal above the ionization potential being absorbed. Prominent absorption lines corresponding to excitation to the laser-dressed 1s3p (23.1 eV, ~6 *fs* classical period) and 1s4p (23.74 eV, ~15 *fs* classical period) states, as well as the ionization potential, are indicated in the figure. Photon energies below 22 eV, including absorption due to the 1s2p state (21.2 eV), were beyond the detection range of the XUV spectrometer and could not be seen in the experiment.

We find that the cycle-averaged positions of the absorption lines follow the intensity profile of the 6 *fs* NIR laser, as indicated in Fig. 1(c). The observed energy shifts at the peak of the laser pulse agree well with recent calculations[10,11] and measurement of the cycle-averaged 1s3p Stark shift[12].

One surprising feature in the measured spectrogram is the fast modulation of the absorption with a period of ~1.3 *fs*, half the laser oscillation period, indicated in Fig. 1(d) for absorption near the unperturbed 1s3p and 1s4p absorption lines. Interestingly, this modulation is present not only near the absorption peaks of the 1s*n*p states, but persists in regions of low absorption (for example, near 22.7 eV and 23.5 eV near zero delay). Such modulations in the transient absorption signal were previously observed using an attosecond pulse train[13], and the authors also noted that the transmitted signal far from any absorption peaks was modulated. These modulations of the absorption probability can be explained by the laser-induced changes to the amplitudes $c_k(t)$ leading to interferences in the electron wavepacket [14-17]. However, previous studies have not considered the effects of the sub-cycle AC Stark shifts.

Due to the broad continuum spectrum of the isolated attosecond pulse, we are able to extract the sub-cycle energy shifts and linewidths of the excited state energy levels. In Fig. 2, we plot the shifts of the central energies and the absorption linewidths of the laser-dressed 1s3p and 1s4p absorption lines, obtained by fitting each absorption line to a Gaussian function for every delay step. We find that the half-cycle dynamics are apparent in each absorption line, but there are differences in the features of different excited states. From the plots, we find that the 1s3p absorption line exhibits a periodic shift and broadening with approximately twice the laser frequency, superimposed on the overall shift on the timescale of the pulse envelope. The sub-cycle shift of the 1s4p energy, however, is substantially reduced in comparison to those of the 1s3p state.

In the transient absorption measurement, the interaction of the atom with the XUV and NIR pulses with a time delay τ_D induces a time-dependent polarization $P(t,\tau_D)$, which emits an electromagnetic field. It is this polarization-induced radiation which is then measured by the XUV spectrometer. The measured spectrum at each time delay is related to the Fourier transform of the polarization, which samples the dynamics induced by the two fields over a longer time period after the XUV excitation, as pointed out in Ref. [18]. We therefore follow the theoretical treatment in Ref. [18], and calculate the absorption from the time-dependent polarization,

$$P(t,\tau_D) = n_{at}\left\langle \Psi(\mathbf{r},t,\tau_D)\middle|\hat{z}\middle|\Psi(\mathbf{r},t,\tau_D)\right\rangle, \qquad (6)$$

where n_{at} is the atomic number density, $\hat{z}$ is the component of the electric dipole operator along the polarization axis of the two fields, and $\left|\Psi(\mathbf{r},t,\tau_D)\right\rangle$ is the time-dependent electron wavefunction in the presence of both XUV and NIR fields.

To calculate $\left|\Psi(\mathbf{r},t,\tau_D)\right\rangle$, we make several assumptions: (1) the NIR pulse has no effect on the ground state $\left|\psi_0(\mathbf{r})\right\rangle$ because of its large binding energy and the low NIR intensity (~10^{12} W/cm^2) and its effects on excited states were treated with second-order perturbation theory, (2) the XUV pulse was treated as a δ-function arriving at time τ_D, which is justified since the XUV

duration is much shorter than the NIR laser cycle, (3) the XUV-atom interaction was treated perturbatively due to the low intensity of the XUV field, and (4) each excited state was treated independently. Under these assumptions, we can calculate the time-dependent electron wavefunction as:

$$\left|\Psi(\mathbf{r},t,\tau_D)\right\rangle \approx \begin{cases} \left|\psi_0(\mathbf{r})\right\rangle e^{-iE_0 t}, t < \tau_D \\ \left|\psi_0(\mathbf{r})\right\rangle e^{-iE_0 t} + d_{a0}\varepsilon_{XUV}(t)\left|c_a^{ion}(t)\right| e^{-i\int_{\tau_D}^{t}[E_a+\delta E_a(t')]dt'} \left|\psi_a(\mathbf{r})\right\rangle , t > \tau_D \end{cases}, \quad (7)$$

where $\left|c_a^{ion}\right|$ describes the reduction in the excited state population due to ionization.

For the excited states of interest, we can calculate α_{1s3p} and γ_{1s3p} (as well as α_{1s4p} and γ_{1s4p}) from tabulated values of transition frequencies and oscillator strengths [19]. From this, we then calculated the sub-cycle AC Stark shift for each state. To calculate the reduction of the populations of the 1s3p and 1s4p states due to ionization, we used the PPT ionization rates [20]. Based on the above assumptions, we calculated $P(t,\tau_D)$ and its Fourier transform $\tilde{P}(\omega,\tau_D)$. The XUV transmission at each delay was then calculated from Beer's law as:

$$T(\omega,\tau_D) = e^{-4\pi L\frac{\omega}{c}\mathrm{Im}\left[\frac{\tilde{P}(\omega,\tau_D)}{\tilde{\varepsilon}_{XUV}(\omega)}\right]}, \quad (8)$$

where L is the interaction length and $\tilde{\varepsilon}_{XUV}(\omega)$ is the XUV spectrum before absorption, which is constant for the δ-function pulse. The photon energy-dependent transmission, calculated separately for 1s3p and 1s4p using the experimental laser parameters, is shown in Figure 3(a). Several qualitative features of the 1s3p and 1s4p absorption are reproduced well, including the overall energy shift and the sub-cycle modulations. In Figures 3(b) and (c), we plot the energy shifts and widths of the laser-dressed 1s3p and 1s4p states, and find that the sub-cycle features in the observed shifts and widths are reproduced quite well by the sub-cycle AC Stark shifts. Figures 3(b) and (c) also show the calculated energy level shift for and width for the 1s3p state when only the ionization is included. In this case, there is no observed energy level shift or sub-cycle modulations in the linewidth, confirming that these features are caused by the sub-cycle AC Stark shift. Although several other features, for example the exact magnitude of the energy level shift and the full-width at half maximum width of the shift profile along the delay axis, cannot be reproduced exactly, these discrepancies likely arise from inaccuracies in the calculation and the approximations we made. For example, the available tabulated dipole matrix elements are limited and couplings to continuum states may not be accurately treated by the PPT model.

Attosecond pulses promise to open new doors in observation and control of electron dynamics as we gain more understanding of quantum mechanical processes on ultrashort timescales. Here, we observe sub-cycle features in the laser-induced Stark shift which occurs on the attosecond timescale. We find that the 1s3p and 1s4p absorption lines in helium are periodically shifted and broadened in the presence of a moderately intense field, which can be reproduced by sub-cycle AC Stark shifts uncovered by the use of isolated attosecond pulses. The observed sub-cycle shift and broadening of the absorption lines of Stark-shifted helium excited

states clearly demonstrate that even bound electrons with characteristic timescales of motion much larger than the laser period can respond nearly instantaneously to a perturbing laser field.

This work is supported by the U. S. Army Research Office, by the U.S. Department of Energy, and by the National Science Foundation.

References

[1] N. B. Delone and V. P. Krainov, Sov. Phys. Usp. **42**, 669 (1999).

[2] A. M. Bonch-Bruevich *et al.*, Sov. Phys. JETP **29**, 82 (1969).

[3] B. H. Bransden and C. J. Joachain, *Physics of Atoms and Molecules* (Pearson, New York, 2003).

[4] D. Normand *et al.*, J. Opt. Soc. Am. B **6**, 1513 (1989).

[5] A. Mysyrowicz *et al.*, Phys. Rev. Lett. **56**, 2748 (1986).

[6] P. C. Becker *et al.*, Phys. Rev. Lett. **60**, 2462 (1988).

[7] X. Feng *et al.*, Phys. Rev. Lett. **103**, 183901 (2009).

[8] H. Wang *et al.*, Phys. Rev. Lett. **105**, 143002 (2010).

[9] S. Gilbertson *et al.*, Phys. Rev. Lett. **105**, 093902 (2010).

[10] M. B. Gaarde *et al.*, Phys. Rev. A **83**, 013419 (2011).

[11] X. M. Tong and N. Toshima, Phys. Rev. A **81**, 063403 (2010).

[12] M. Swoboda *et al.*, Phys. Rev. Lett. **104**, 103003 (2010).

[13] M. Holler *et al.*, Phys. Rev. Lett. **106**, 123601 (2011).

[14] P. Johnsson *et al.*, Phy. Rev. Lett. **95**, 013001 (2005).

[15] P. Riviere *et al.*, New J. Phys **11**, 053011 (2009).

[16] P. Ranitovic *et al.*, New J. Phys. **12**, 013008 (2010).

[17] X. M. Tong *et al.*, Phys. Rev. A **81**, 021404 (2010).

[18] R. Santra *et al.*, Phys. Rev. A **83**, 033405 (2011).

[19] G. W. F. Drake, in *Springer Handbook of Atomic, Molecular and Optical Physics*, edited by G. W. F. Drake (Springer, New York 2006).

[20] A. M. Perelomov, V. S. Popov, and M. B. Terent'ev, Sov. Phys. JETP **23**, 924 (1966).

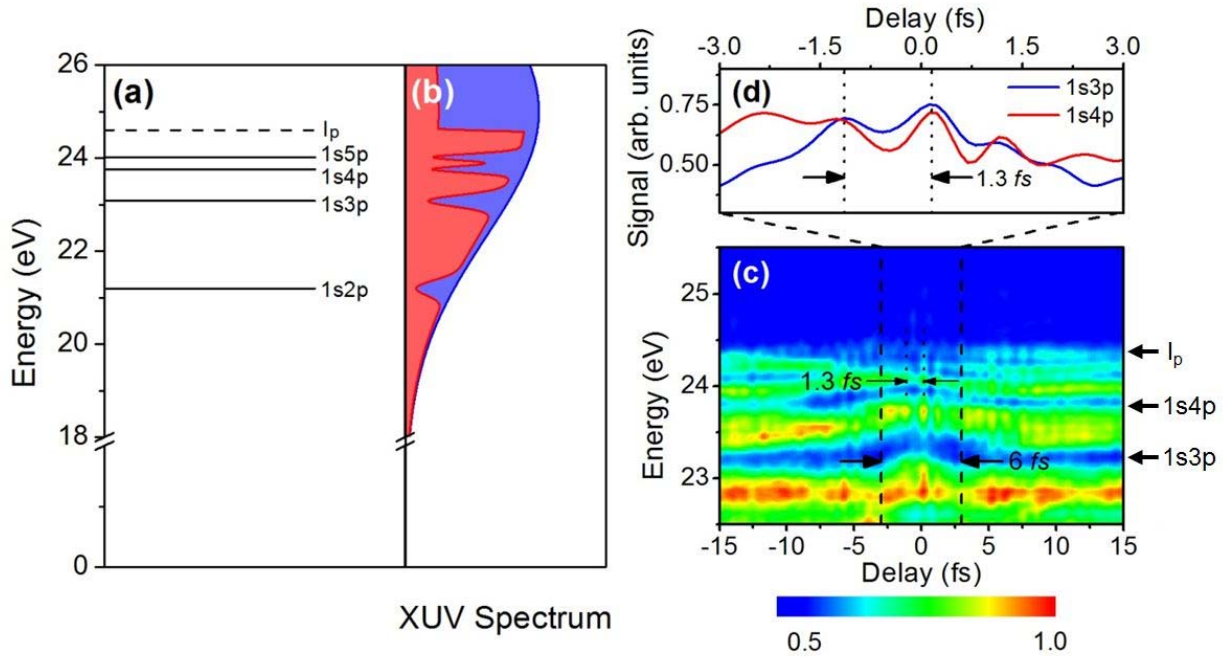

Fig. 1 Helium 1s*n*p absorption. (a) Energy levels of the helium excited states of interest with energies relative to the ground state. The ionization potential (I_p) is 24.6 eV. (b) Schematic of the XUV attosecond pulse spectrum before (blue) and after (red) absorption. (c) Transmitted XUV spectrum as a function of the time delay between the two pulses. The blue color indicates low transmission (high absorption). Negative delays indicate that the attosecond pulse arrives on the target before the NIR laser. (d) Lineouts of the transmitted XUV signal near the unperturbed 1s3p and 1s4p absorption lines near zero delay, indicating the half-cycle periodicity.

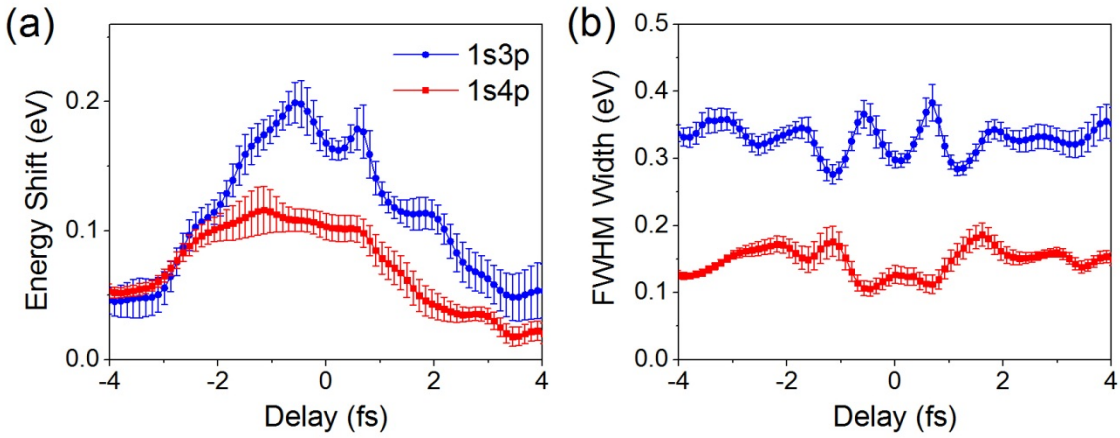

Fig. 2 Absorption line dynamics in laser-dressed excited states. (a) Energy shift and (b) full-width at half-maximum of the 1s3p and 1s4p absorption lines as a function of the time delay. Error bars indicate 99% confidence bands of each parameter in a Gaussian fit. The 1s3p energy level shows an overall shift on a 6 *fs* timescale with sub-cycle shifting and broadening at positive delays. Modulations of the 1s4p energy and width are substantially smaller.

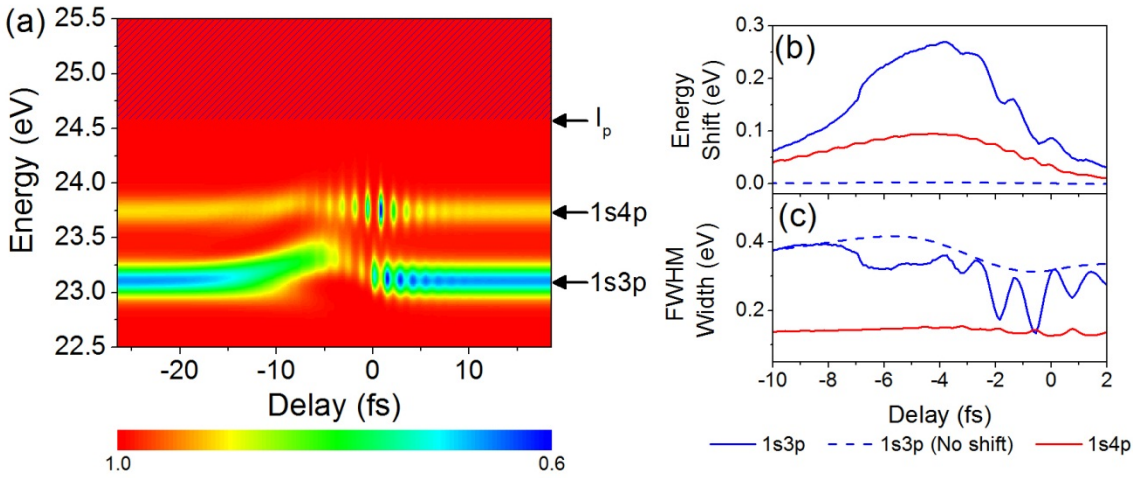

Fig. 3 Transient absorption calculation. (a) Calculated transmitted spectrum as a function of the time delay between the XUV pulse and NIR field. The absorption is calculated for each state individually and added together to obtain the figure. The shaded region above the ionization potential (24.6 eV) is not included in the calculation, but is included here for comparison with Fig. 1(c). (b) Calculated energy level shifts and (c) widths for the laser-dressed 1s3p (solid blue) and 1s4p (solid red) states, as well as the energy level shift and width for the 1s3p state due only to ionization (dashed blue, $\alpha_{1s3p} = \gamma_{1s3p} = 0$).